JOURNAL OF COLLOID AND INTERFACE SCIENCE 175, 46–56 (1995)

Phase Separation of Mixtures of Colloidal Boehmite Rods and Flexible Polymer

JOHAN BUITENHUIS, LIESBETH N. DONSELAAR, PAUL A. BUINING, ALAIN STROOBANTS, AND HENK N. W. LEKKERKERKER*

Van 't Hoff Laboratory, Utrecht University, Padualaan 8, 3584 CH Utrecht, The Netherlands

Received September 7, 1994; accepted February 24, 1995

Phase separation experiments have been performed on mixtures of colloidal polyisobutene grafted boehmite rods and flexible polymers. Two systems of rods have been studied, one with an average length and diameter of 71 nm and 11.1 nm, and the other with an average length and diameter of 253 nm and 9.4 nm. The polymers used have molecular weights varying from 35 to 186 kg mol^{-1}, leading to radii of gyration of 5.9 to 20 nm. Bi- and triphasic equilibria involving a dilute isotropic phase, a concentrated isotropic phase, and a nematic phase are observed. The phase behavior is compared to a recent theory, which is an extension of the treatment for sphere/polymer mixtures (H. N. W. Lekkerkerker *et al., Europhys. Lett.* 20, 559 (1992)). The main features of the phase behavior can be understood on the basis of this simple theory. There remain significant discrepancies between theory and experiment which are attributed to the limitations of the theory on the one hand and to the polydispersity of the colloidal rods and the formation of metastable and nonequilibrium states such as colloidal gels and glasses on the other hand.

Key Words: boehmite; polymer; phase separation; colloidal rods; nematic phase.

1. INTRODUCTION

Mixtures of colloidal particles with nonadsorbing flexible polymer can phase separate into a colloid rich and a colloid poor phase, due to the so-called depletion interaction. This interaction arises from the asymmetric distribution of polymer molecules around a colloidal particle when the surface to surface distance between two colloidal particles is smaller than the radius of gyration of the polymer molecules. Consequences of this interaction were already observed over half a century ago in the creaming of rubber latex (1–3), although the possibility of a depletion force was not recognized at that time. Asakura and Oosawa (4, 5) were the first to clearly recognize that dissolved polymer may induce an attraction between colloidal particles and provided a simple but useful theory for this. Their theory was soon substantiated by direct experimental evidence by Sieglaff (6) for a phase separation resulting from a depletion interaction. After almost two decades of limited activity, a series of important experimental and theoretical studies were performed on mixtures of colloidal spheres and polymer coils (7–19). An important result of these studies was the observation of different structures for the coexisting phases (12, 14–17), which can be considered as the colloidal analogues for the molecular gas, liquid, and solid phases. The last phase can have either a crystalline or an amorphous (glass or gel) structure (15, 17). The relevant parameter determining the type of phase behavior was found to be the range of the effective colloidal attraction, which is determined by the ratio of the radius of the polymer coil to the radius of the colloidal sphere (12, 14, 15). Under certain conditions a three-phase region in which a colloidal gas, liquid, and crystal coexist is predicted to occur (20). Recently such triphasic equilibria have been reported (21, 22).

All of the studies described in the previous paragraphs are limited to spherical colloidal particles. A part from some interesting work focusing on the purification of (rodlike) virus particles (23–27), the only studies devoted to other particle shapes are restricted to mixtures of rigid rodlike polymers and flexible polymers (28–32). The principle of this phase separation is similar to that for the sphere/coil mixtures; nevertheless, there has been (almost) no interaction between the two lines of study. The commonly used theoretical description of the rod/coil mixtures is given in terms of a lattice model by Flory (33).

A restriction of the experimental and theoretical work on rigid and flexible polymers is that the diameter of the coils is always larger than that of the rods. Here we present a study on mixtures of colloidal rods and flexible polymers where the coil diameter of the flexible polymer is of the same order of magnitude as the diameter of the rods. This diameter ratio turns out to be important for the phase behavior.

The colloidal rods used in this study are boehmite parti-

* To whom correspondence should be addressed.

0021-9797/95 $12.00

cles, sterically stabilized with end-functionalized polyisobutene (34). The synthesis of these particles is performed according to a procedure that was recently developed in our laboratory (35, 36). Phase diagrams for two systems are studied here. The first system consists of boehmite rods with an average length of 71 nm and an average diameter of 11.1 nm dispersed in *o*-dichlorobenzene, with polystyrene of 35 kg mol^{-1} (effective diameter $\approx$13 nm) as the added polymer. The boehmite rods of the second system have an average length of 253 nm and an average diameter of 9.4 nm and are dispersed in cyclohexane. The phase separation in this system is studied with added polydimethylsiloxane of molar masses 65, 92, and 186 kg mol^{-1}. The corresponding effective diameters of the polymer coils are estimated to be 24, 29, and 45 nm, respectively. A rich phase behavior is observed, in particular for the first system, which exhibits triphasic equilibria of two isotropic and one nematic phase. The measured phase diagrams are compared to predictions for the phase behavior of the mixed rod/coil system based on a theory (37) which is an extension of the treatment for sphere/coil systems (20). The basic principles and the main results of this theory for the rod/coil system are outlined in the next section.

2. THEORY

The theory of the phase behavior of mixtures of rodlike colloid particles and polymer molecules that is used in this paper is a direct extension of the work of Lekkerkerker *et al.* (20) on the phase behavior of spherical colloidal particles and polymer molecules. Here we only give a brief outline of the theory; a detailed discussion can be found elsewhere (37).

The polymer molecules are treated as freely interpenetrable coils of diameter σ, of which the centers of mass cannot approach the (nonadsorbing) surface of the colloidal particles within closer than a distance $\sigma/2$. As the polymer coils do not feel each other, the pure polymer solution will behave thermodynamically ideally. The colloidal particles themselves are modeled as hard spherocylinders consisting of cylinders of diameter D and length L capped with two hemispheres. Using a mean field treatment (20, 37, 38) the Helmholtz free energy for this system can be written as

$$F(N_C, N_p, V, T, [f]) = F_C(N_C, V, T, [f]) + F_p(N_p, \langle V_{free}\rangle_0, T). \quad [1]$$

Here F_C is the Helmholtz free energy of a pure system of N_C colloidal rods in a volume V at a temperature T and F_p is the Helmholtz free energy of N_p polymer coil in a volume $\langle V_{free}\rangle_0$, the average free volume in the pure system of colloidal rods. Further, $f(\mathbf{u})$ is the orientation distribution function, which gives the probability of finding a rod with an orientation characterized by a unit vector $\mathbf{u}$. To make progress we need expressions for the Helmholtz free energies and the average free volume. Both quantities can be obtained using Scaled Particle Theory (39, 40). The resulting expression for F must be minimized with respect to the orientation distribution function. This results in two types of solution corresponding to an isotropic and a nematic phase, respectively. The phase transitions in the system can now be located by solving the coexistence conditions for the chemical potentials and the pressure. This leads to three types of phase behavior, which are illustrated in Fig. 1 in a representation showing colloid volume fraction ϕ_C against polymer coil volume fraction ϕ_p.

Depending on the length-to-width ratio of the rod-like particles and the ratio of the polymer diameter and rod diameter we find three types of phase behavior:

(a) A phase diagram with two isotropic phases ("dilute" and "concentrated," the equivalent of vapour and liquid) and a nematic phase. This phase behavior is predicted to occur for mixtures of relatively short rods and large polymers.

(b) A phase diagram with an isotropic and a nematic phase. This phase behavior is predicted to occur for rods with intermediate length-to-width ratios and intermediate polymer to rod diameter ratios.

(c) A phase diagram with one isotropic phase and two nematic phases differing in concentration. This phase behavior is predicted to occur for long rodlike particles and relatively small polymer molecules.

The occurrence of the three different regimes as a function of the geometrical parameters L/D and σ/D is shown in Fig. 2.

3. MATERIALS AND METHODS

3.1. Synthesis of the Rods

Both systems of boehmite rods are synthesized and grafted with polyisobutene modified with an anchor group (34) according to Buining *et al.* (35, 36), with some minor modifications.

ASB33g (average length 71 nm, average diameter 11.1 nm). Colloidal boehmite rods were synthesized by adding 91.5 g aluminium tri-*sec*-butoxide (ASB) to 2 liters HCl (0.037 *M*) while stirring. After three days of continuous stirring, the turbid liquid was treated hydrothermally at 150°C for 20 h. This hydrothermal treatment was performed without the usual rotation of the autoclaves, which were left at rest for about 90 min before the autoclaves were put in the oven. This minor change turned out to give an important reduction of the degree of clustering, as was demonstrated

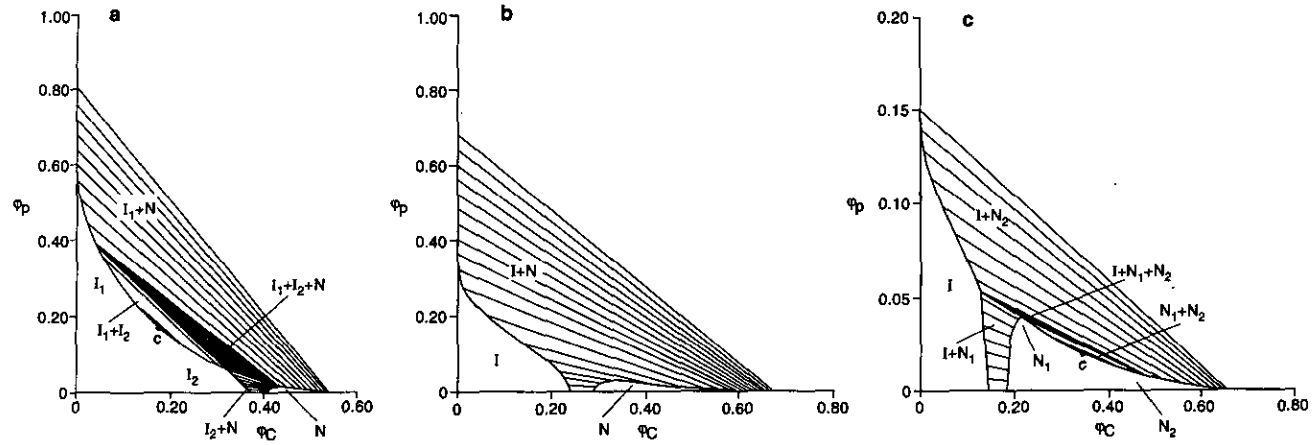

FIG. 1. Phase diagrams for rodlike colloid + flexible polymer mixtures showing colloid volume fraction ϕ_C against polymer coil volume fraction in the system ϕ_p: (a) $L/D = 5$, $\sigma/D = 0.80$; (b) $L/D = 10$, $\sigma/D = 0.65$; (c) $L/D = 20$, $\sigma/D = 0.50$. I and N refer to isotropic and nematic phases respectively. Tie lines are shown in the two-phase regions. The critical point is indicated by c.

by electron microscopy and static light scattering. After the hydrothermal treatment, the dispersion was dialyzed against flowing deionized water for 13 days.

Subsequently, the particles were transferred to propanol by distillation, keeping the boehmite concentration below 1.6 g/liter. To 3.5 liters propanol sol, 2.8 liters of a solution of 10 g polyisobutene in 1 liter tetrahydrofuran was added. Stepwise addition of toluene and distillation yielded a dispersion in toluene, which was then concentrated to about 10 g/liter. After cooling, the dispersion was exposed to ultrasonication for 15 min, resulting in a reduction of its turbidity. After 2 days, the excess polyisobutene was removed in two steps: centrifugation at 10,000 rpm followed by redispersion in cyclohexane. Accumulated dust was removed by 2 h centrifugation at 2000 rpm, yielding a stable, dark red stock dispersion of 9.39 w/w%. The stock dispersion in cyclohexane was concentrated by evaporation at room temperature under a nitrogen flow, until a very viscous dispersion was obtained. The concentrated sample was stirred for at least two weeks, after which *o*-dichlorobenzene was added. Finally, evaporation of the cyclohexane yielded a dispersion in *o*-dichlorobenzene.

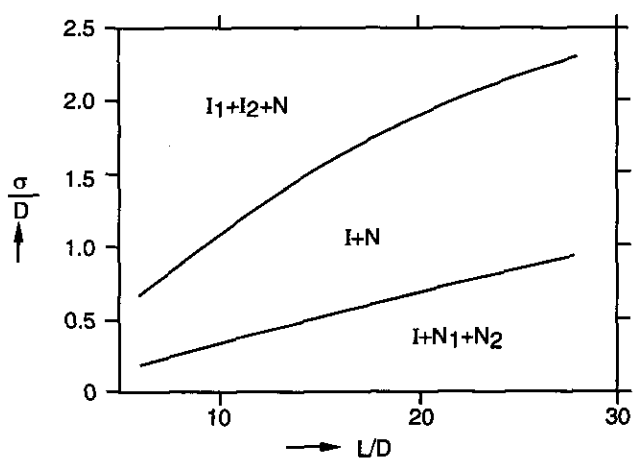

FIG. 2. Dependence of the type of phase behavior or rodlike colloid + flexible polymer mixtures on the size parameters of the colloid and polymer. $I_1 + I_2 + N$: phase diagram with two isotropic phases and a nematic phase; $I + N$: phase diagram with an isotropic and a nematic phase; $I + N_1 + N_2$: phase diagram with one isotropic and two nematic phases.

The treatment described above was first performed on a small test sample (ASB33g-1) and subsequently a larger amount of dispersion was used (ASB33g-2). Three months later, a third amount of sample was concentrated and transferred to *o*-dichlorobenzene (ASB33g-3). Although the three batches were treated in as much the same way as possible, a significant difference in dispersion behavior was observed. The batches ASB33g-1 and ASB33g-2 started to form gellike clots at a volume fraction of about 18%, whereas the batch ASB33g-3 remained homogeneous up to a volume fraction of about 28.5%, above which an isotropic–nematic phase separation occurred. The origin of this completely different behavior is unclear. Further experiments focused on ASB33g-3, which will be denoted as ASB33g.

ASBIP13g (average length 253 nm, average diameter 9.4 nm). Colloidal boehmite rods were synthesized by adding 97.2 g aluminium tri-*sec*-butoxide (ASB) and 75.6 g aluminium tri-*iso*-propoxide (AIP) to 5 liters HCl (0.086 *M*) while stirring. After a week of continuous stirring, the weakly turbid solution was treated hydrothermally at 150°C for 20 h under continuous rotation of the autoclaves. After cooling, the boehmite dispersion was dialyzed for 1 week against streaming deionized water.

A volume of propanol equal to four times the volume of the boehmite dispersion was added to it under ultrasonication, followed by azeotropic distillation until a propanol dis-

persion was obtained with a concentration of 3.6 g/liter. To 1 liter propanol sol, 0.4 liter of a solution of 10 g polyisobutene in 1 liter tetrahydrofuran was added under ultrasonication. Stepwise addition of toluene and distillation yielded a dispersion in toluene. The excess polyisobutene was removed by centrifugation at 10,000 rpm followed by redispersion in cyclohexane. The resulting dispersion was concentrated by evaporation of the solvent at room temperature, by bubbling nitrogen through it.

3.2. *Characterization of the Rod Dispersions*

Particle density. The particle density was determined by comparing the weight of 10 ml of a dispersion of known concentration in cyclohexane with that of 10 ml of cyclohexane in the same measuring flask. The weight/weight concentration was determined by weighing a small amount of dispersion, and then drying it to constant weight under an IR-lamp.

The average density of the particles is 1.97 ± 0.07 g/ml for the ASB33g system and 2.11 ± 0.07 g/ml for the ASBIP13g system. These densities were used to calculate the volume fractions from the measured weight/weight concentrations.

Electron microscopy. Electron photomicrographs were made with a Philips CM10 transmission microscope. The samples for the ASBIP13g system were prepared by dipping common formvar coated copper grids in a dilute dispersion, and the samples for the ASB33g system were prepared by spraying or dropping a very dilute dispersion on 300 mesh copper grids coated with a thin carbon film. The thin carbon film was not stabilized by a polymer film, to reduce the background and thereby increase the contrast in the electron microscope. In this way enough contrast was obtained, without having to work out of focus, as was necessary for the ASBIP13g system.

For the ASB33g system, the particle dimensions could be obtained directly from the electron microscopy photographs, a representative example of which is shown in Fig. 3a. The length and diameter of the particles is determined with an interactive image analysis system. For particles with an irregular structure the diameter was estimated. The average dimensions with their standard deviations and the correlation coefficient are given in Table 1. Note that the actual diameter in the dispersion may deviate somewhat from the electron microscopy diameter because of swelling of the steric stabilization layer.

A representative electron microscopy photograph for the ASBIP13g system is given in Fig. 3b, clearly showing aggregated bundles of rods. Consequently we were not able to determine the particle dimensions from the electron microscopy photographs of ASBIP13g directly. It was possible, however, to determine the dimensions of the particles from electron microscopy photographs before the grafting procedure. The dimensions for the grafted particles were then obtained by making a correction for the thickness of the grafting layer, which was estimated from the particle density of 2.11 g/ml using a boehmite density of 3 g/ml and a grafting layer density of 1 g/ml. It is noted that, because of the aggregates and the possible breaking of particles during the grafting procedure, this gives only a rough estimate of the particle dimensions. The resulting dimensions are given in Table 1.

3.3. *The Flexible Polymers*

The polystyrene (PS) used was a standard sample obtained from Pressure Chemical Co. (Pittsburgh, PA) with a reported molar mass of 35K and $M_w/M_n < 1.06$. The radius of gyration (R_g) of the PS in *o*-dichlorobenzene was determined by multiplying its value in a theta solvent (41) by the coil expansion. The latter was obtained from the empirical scaling function determined by Berry (42) using the second virial coefficient of PS in *o*-dichlorobenzene as measured by Krigbaum *et al.* (43).

The three polydimethylsiloxane (PDMS) samples were general purpose silicones (trimethylsiloxy terminated) from ABCR GmbH&Co, Karlsruhe, Germany. For the molar masses as determined by gel permeation chromatography (GPC) in tetrahydrofuran and/or by static light scattering (Zimm plot) in toluene, the values 65K, 92K, and 186K were obtained. For the 92K and 186K PDMS, the R_g's in cyclohexane were determined from static light scattering (Zimm plots), while the R_g of the 65K PDMS was obtained by extrapolation from the other two assuming proportionality to $M_w^{3/5}$.

Table 2 shows an overview of the relevant parameters for the four polymer samples used. In order to compare the measured phase diagrams with calculated diagrams an effective polymer diameter $\sigma = 2.25\ R_g$ was used following de Hek and Vrij (13). Although this relation was derived for polymers between parallel plates in a theta solvent, we consider that it provides a reasonable estimate of σ for the case good solvents used here.

3.4. *Methods*

In the ASBIP13g system, polymer concentrations leading to phase separation were obtained by preparing a series of boehmite + PDMS mixtures in cyclohexane with increasing PDMS concentrations. Subsequently, the limiting polymer concentrations (c_{lim}) were determined to within a few percent with small concentration steps.

For the ASB33g system a different procedure was followed, as the amount of sample was limited. Two concentrated boehmite + PS mixtures in *o*-dichlorobenzene were diluted in small steps either with the pure solvent or with a

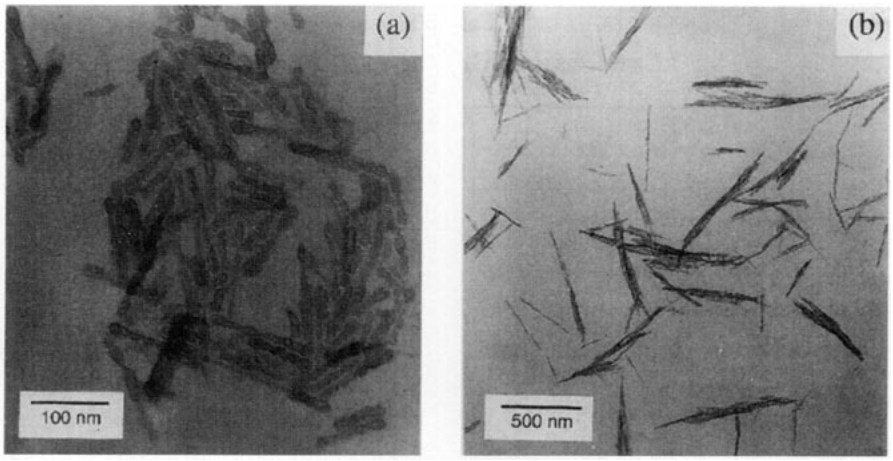

FIG. 3. Electron microscopy photographs of (a) ASB33g and (b) ASBIP13g.

dispersion of the same concentration as in the mixture. In the one-phase region of the phase diagram, additional PS was added after which two dilution series with solvent were made. At the end of both double dilution series, the overall concentration in the two sample tubes (polymer + rods) was determined and was found to agree within a few percent with the concentrations as calculated from the subsequent additions.

Using the strong optical absorption of the ASB33g sample, resulting in dark red samples at higher concentrations, the boehmite concentration in the coexisting isotropic phases could be estimated by comparison of its color to a calibration series. In combination with an estimate of the relative volume of the coexisting phases, estimates of the concentrations in the much more turbid nematic phases could also be made. The presence of the polymer did not appear to influence these estimates; this could be checked for some fully isotropic samples with polymer concentrations close to the phase separation concentration.

All phase separation experiments were performed at room temperature. After preparation, the samples were thoroughly mixed with a vortex mixer. Birefringent phases were identified using crossed polaroid filters and a focused lamp.

TABLE 1
Characterization of the Rod Systems

	ASB33g	ASBIP13g
Average length (nm)	71	253
Standard deviation of the length (nm)	31	—
Average width (nm)	11.1	9.4
Standard deviation of the width (nm)	2.4	—
Correlation coefficient	0.40	—
Average particle density (g ml^{-1})	1.97 ± 0.07	2.11 ± 0.07

4. RESULTS

4.1. ASB33g + PS in o-Dichlorobenzene

We first studied the phase behavior of the ASB33g system without added polymer. A 27.4% v/v sample did not phase separate on standing for several months, whereas at 29.2% v/v a phase separation was observed in an isotropic phase of 28.5 ± 0.3% v/v and a highly viscous nematic phase of 31 ± 1% v/v. It took about two days for the phase separation to be completed. Upon cessation of the phase stirring the birefringence pattern of the system remained virtually unchanged for several hours after which the phase separation process became visible between crossed polars. In Fig. 4 we give a polarization microscopy photograph of such a phase separated sample.

Subsequently, the phase behavior for the ASB33g system

TABLE 2
Characterization of the Polymer Samples

			$\langle R_g^2 \rangle^{1/2}$ (nm)		
Polymer	M_w (kg mol^{-1})	M_w/M_n	θ-solvent	Used solvent	σ (nm)
PDMS	65[a]	1.49[a]	6.8[d]	10.5[f]	24
PDMS	92[a,b]	1.30[a]	8.1[d]	13[b]	29
PDMS	186[b]	—	11.5[d]	20[b]	45
PS	35[c]	<1.06[c]	5.2[e]	5.9[g]	13.3

[a] Gel permeation chromatography.
[b] Static light scattering (Zimm plot).
[c] Value from Pressure Chemical Company.
[d] Value taken from Ref. (41).
[e] Value taken from Ref. (42).
[f] Extrapolated using $R_g \sim M_w^{3/5}$.
[g] Calculated from the value in θ-solvent using the coil expansion factor (see section 3.3).

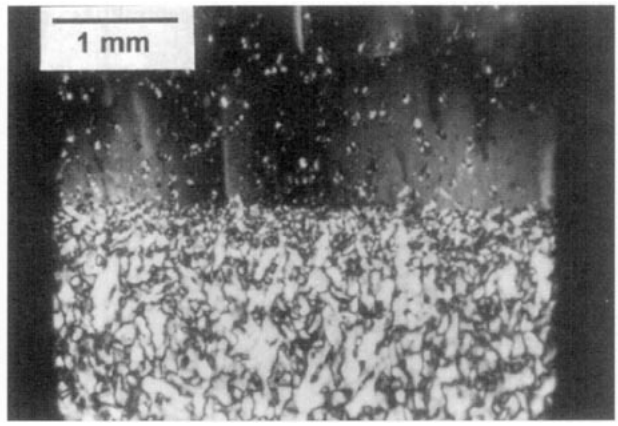

FIG. 4. Polarization microscopy photograph of a phase separated ASB33g sample showing the coexisting phases: nematic (lower half) and isotropic (upper half). Some nematic droplets are still settling, and a thin layer of nematic phase, which sedimented against a side-wall of the flat capillary (4 × 0.2 mm), results in a weakly birefringent background for the isotropic phase.

with 35K PS was studied. Several coexisting phases were observed for this system, of which the most important are a dilute isotropic phase (I_1), a concentrated isotropic phase (I_2), and a highly birefringent (viscous nematic) phase (N). When the sample tube was tilted, both isotropic phases flowed immediately, while it took the nematic phase about 15 to 60 min to complete its flow. Almost all phase separations were completed within two days. An illustration of a I_2N phase separation is given in Fig. 5, showing a photograph of a sample tube between crossed polars, just after mixing (Fig. 5a) and after the phase separation is completed (Fig. 5b). A coarse and cloudy birefringence pattern of the sample directly after mixing and a more fine and sharp appearance after phase separation are generally observed. An example of an I_1 I_2 N three-phase equilibrium is shown in Fig. 6.

An overview of the results is shown in the phase diagram in Fig. 7. Apart from the coexisting phases already discussed, some additional states were observed. As the polymer concentration increased a relatively colorless and turbid amorphous sediment first separated from the dispersion. Using the same combination of static and dynamic light scattering as described in Ref. (44) we were able to show that the sediment consists almost entirely of clusters that are present in the original Boehmite dispersion (45). The other additional states were found when we followed the dilution line starting at ϕ_C = 23.4% v/v and [PS] = 28.4 g/liter toward the origin of the diagram in Fig. 7. At the starting point a gel-like, sticky, and very turbid dispersion was obtained after thoroughly mixing the sample. Subsequent phase separation resulted in an upper phase with a very low boehmite concentration (<0.75% v/v) and a turbid gel or glass-like lower phase that did not flow within an hour after tilting the sample tube. Neglecting the boehmite in the upper phase, the boehmite concentration in the lower phase was estimated to be 33% v/v. Diluting the sample to ϕ_C = 18.8% v/v and [PS] = 22.9 g/liter again resulted in an upper phase with a very low boehmite concentration, but now the lower phase was birefringent. This lower phase again did not flow within 1 h and is therefore denoted as a nematic glass. Its concentration is about 38% v/v. Upon further dilution, the boehmite concentration in the upper phase increased and the lower phase became less viscous and developed a finer and sharper birefringence pattern. At the point where the lower phase completed its flow within 1 h after the sample tube was tilted, it is denoted as a nematic. At this point, the boehmite concentration in the upper phase was estimated to be 2 ± 0.5% v/v. With further dilution up to the boundary of the three phase region, the boehmite concentration in the upper phase reached the value 3.5 ± 1% v/v.

Diluting the system through the three-phase region at first caused the volume of the I_2 phase to increase while the volume of the N phase decreased. In the lower half of the

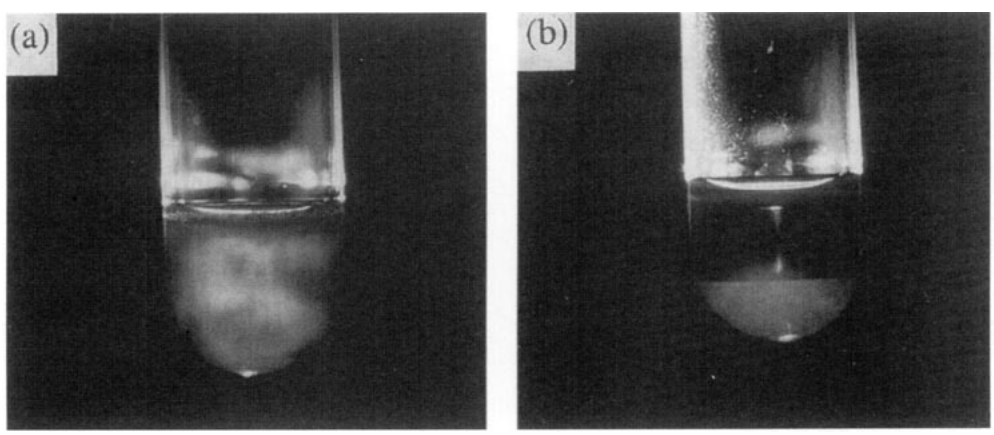

FIG. 5. Photograph of the ASB33g sample with ϕ_C = 23.4% and [PS] = 13.3 g/liter between crossed polars: (a) just after mixing, and (b) after phase separation.

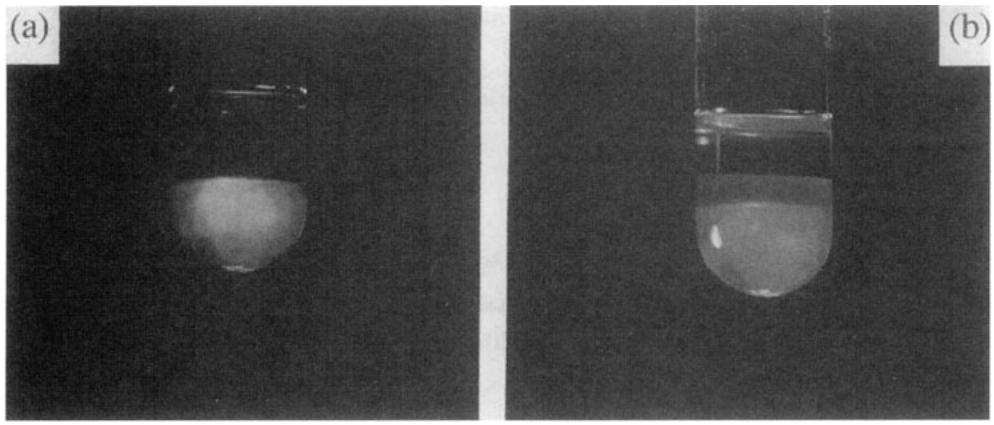

FIG. 6. Photograph of the ASB33g sample with ϕ_C = 20.6% and [PS] = 18.0 g/liter. (a) Between crossed polars. (b) To make the two isotropic phases visible, an additional equilibrated lateral illumination of the sample was used.

three phase region, however, the concentrations of the I_1 and the I_2 phases approached each other, together with a slow decrease of the remaining volume of the N phase. This scenario was also observed along other dilution lines.

However, different behavior was observed when the three-phase region was scanned as a function of the polymer concentration at a colloid concentration fixed at ϕ_C = 23.4% v/v. Upon lowering the polymer concentration, the boehmite concentration in the I_1 phase remained constant at 3 ± 1% v/v while its volume decreased until the two phase I_2N region was entered.

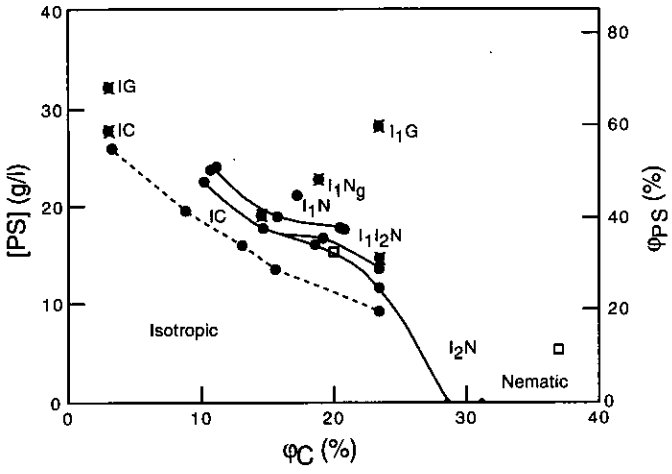

FIG. 7. Observed phases for ASB33g dispersions in *o*-dichlorobenzene with 35k PS added, plotted as a function of the boehmite volume fraction ϕ_C and the polymer concentration, which is given in g/liter as well as the coil volume fraction. Different phases and states are denoted as: I isotropic, N nematic, G glass or gel, N_g 'nematic' (i.e., birefringent) glass or gel, and C cluster sediment. The solid dots denote measured phase boundaries, the asterisks denote single samples or starting points of a dilution series, and the open squares denote the estimated coexisting phases for the sample with ϕ_C = 23.4% and [PS] = 13.3 g/liter. The drawn lines are cubic spline fits for the major phase boundaries, and the dotted line connects limiting concentrations for a cluster sediment (IC coexistence).

4.2. ASBIP13g + PDMS in Cyclohexane

An isotropic nematic phase separation was observed in the boehmite dispersion without added polymer over a rather wide concentration range (7–17% v/v). The volume of the nematic phase seemed to reach a stable value within a week, but a very slow steady change was observed over a long time. Polarization microscopy yielded nematic textures similar to those in Ref. (46). The corresponding isotropic and nematic concentrations as well as the relative amount of nematic phase are plotted as a function of the overall concentration of the dispersion in Fig. 8. The wide biphasic gap and the behaviour of the coexisting concentrations can be attributed to polydispersity effects, as discussed in Ref. (46). For boehmite concentrations exceeding 17% v/v, the dispersion became highly viscous (gel-like) and the isotropic–nematic phase transition was arrested. The dashed lines in Fig. 8a are extrapolations using the results in Fig. 8b to estimate the limiting volume fraction at which the whole system would have become nematic if the isotropic–nematic phase transition were not kinetically arrested.

Phase separation experiments were performed by adding 65, 92, and 186 kg mol^{-1} PDMS to ASBIP13g dispersions with concentration up to the point where the isotropic–nematic phase separation occurred in the pure system. After the addition of a sufficient amount of polymer and thoroughly mixing the samples, a phase separation, in a turbid concentrated and a more clear dilute phase, occurred within a few hours to a few days. The concentrated phases had a rigid structure and are highly viscous. In contrast the nematic phases that occur in pure boehmite systems always completed their flow within 10 s after the sample tube was tilted.

It is remarkable that some of the concentrated phases were birefringent and others were not. The concentrated phases for the samples with added 186K PDMS were all birefringent, whereas the samples with added 65K and 92K PDMS only gave birefringent concentrated phases at the highest boehm-

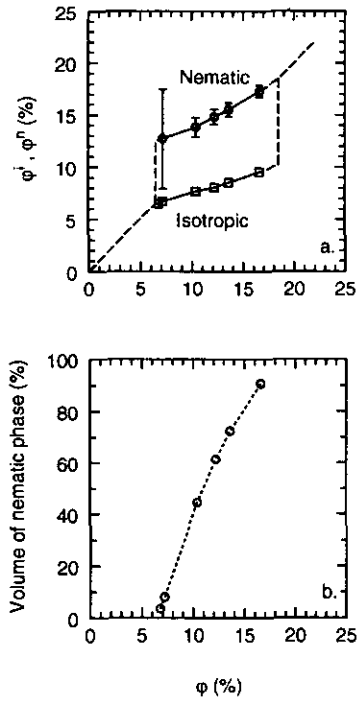

FIG. 8. Isotropic nematic phase separation of ASBIP13g without added polymer. (a) Volume fractions of the coexisting isotropic and nematic phases as a function of the overall volume fraction. (b) Relative volume of the nematic phase as a function of the overall volume fraction.

ite concentration used (5.3% v/v). On average, the birefringent concentrated phases flowed a little faster and were somewhat less turbid than the nonbirefringent concentrated phases.

The limiting polymer concentrations (c_{lim}) for phase separation are given in Fig. 9. It is found that the polymer concentration needed for phase separation decreases with increasing molar mass as well as with increasing volume fraction of the rods. This behavior is similar to depletion phase separation of spherical colloid–flexible polymer mixtures. It seems that the limiting polymer concentration for 65K and 92K PDMS shows a change of slope at the point where the character of the concentrated phase changes from amorphous isotropic to ordered birefringent. This may be a coincidence, but we note that the curve for 186K PDMS, where the concentration phase is birefringent for all ϕ_C, does not show such a change in slope.

An interesting observation was made on a sample with a polymer concentration somewhat above c_{lim}. Here the concentrated coexisting phase is formed from an initial gel-like lower phase with a large volume which then shrinks to a much smaller volume. This is in contrast to the usual case, where the relatively small volume of the concentrated phase forms directly out of the dilute phase (like sediment formation). This observation seems similar to the phenomenon described in a recent work on the gel state in depletion experiments with colloidal spheres at high polymer concentration (47).

5. DISCUSSION AND COMPARISON TO THEORY

5.1. ASB33g + PS in o-Dichlorobenzene

The phase diagram calculated with the theory outlined in Section 2 with the parameters relevant for the system consisting of boehmite rods ASB33g ($\gamma = (L + D)/D = 6.4$) with 35K PS ($q = \sigma/D = 1.2$) is given in Fig. 10a. The disagreement with the experimental results presented in Fig. 7 is manifest. This disagreement may be due to the limitations and approximations of the theoretical treatment as well as to the more complex nature of the experimental system in comparison with the highly idealized model assumed in the theory. This makes an appropriate choice of parameters somewhat ambiguous, a matter not without consequence. For example, simply assuming a somewhat smaller effective polymer diameter already gives a much better agreement between theory and experiment as is evident from the theoretical phase diagram for $\gamma = 6.4$ and $q = 0.8$ presented in Fig. 10b.

As discussed in section 4.1, the I_1 and I_2 concentrations approach each other in the lower half of the three-phase region. This provides evidence for the fact that the polydispersity of the rods, like in the case of the pure rod dispersion (46), again plays an important role in the phase behavior. Indeed, according to the phase rule in a ternary mixture at fixed temperature and (assumed) constant solvent activity, the concentrations of the coexisting phases in the three-phase

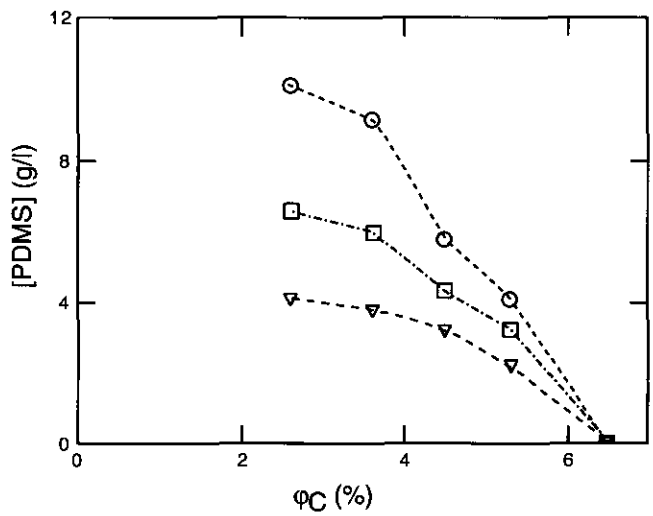

FIG. 9. Limiting polymer concentrations for phase separation of the ASBIP13g sample in cyclohexane with polydimethylsiloxane as polymer. The different structures of the coexisting concentrated phases are discussed in the text. Circles 65K PDMS, squares 92K PDMS, triangles 186K PDMS.

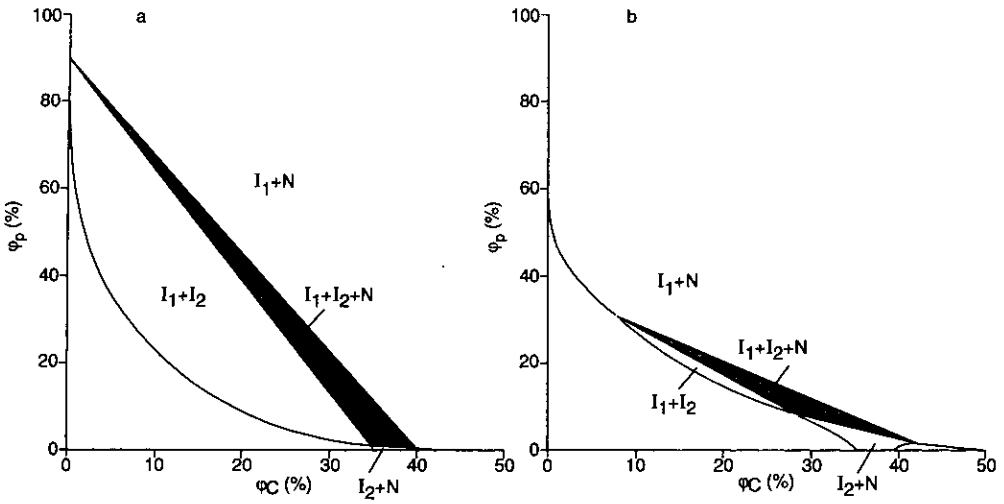

FIG. 10. Theoretical phase diagrams for a system of rodlike colloidal particles and flexible polymers (a) $\gamma = 6.4$ and $q = 1.2$ (b) $\gamma = 6.4$ and $q = 0.8$.

region are constant. In order to understand why this leads to the disappearance of the I_1 I_2 region from the phase diagram, as experimentally observed, a calculation is required in which the polydispersity of the rods is taken into account by representing them at least as a bidisperse system.

In addition to the isotropic and nematic phases, gel or glass states, not considered in the theory, are found at high polymer concentrations. This behavior resembles (some of) the results of a recent study on the gel state in colloidal sphere/polymer mixtures (47). Apparently, at high polymer concentrations the attractions are too strong to allow the system to reach its equilibrium state. This might also explain the change from the nonbirefringent gel or glass state which appears at the highest polymer concentrations, via a birefringent nematic gel or glass state at somewhat lower polymer concentrations to a flowing birefringent nematic phase at still lower polymer concentrations.

5.2. *ASBIP13g + PDMS in Cyclohexane*

The theoretical phase diagrams calculated with the parameters relevant for the system consisting of boehmite rods ASBIP13g ($\gamma = (L + D)/D = 27$) with 65k, 92k and 186k PDMS ($q = \sigma/D = 2.5$, 3.1 and 4.8) are presented in Fig. 11. To facilitate the comparison between theory and experiment, the experimental results given in Fig. 9 are replotted in Fig. 12, where the polymer concentration is now given in terms of volume fraction of the polymer coils. Clearly, the phase behavior predicted by theory shows significant discrepancies with the experimental results. In addition to the effect of polydispersity of the rods, not taken into account in the theory, the large difference between theoretical and experimental phase behavior is probably due to the inadequacy of the theory to deal with systems where the polymer diameter is significantly larger than the rod diameter. It is suspected that this leads to an overestimation of the I_1I_2 region in the calculated phase diagrams.

Another aspect that has to be taken into account is the possibility of the formation of gel or glass states. As indicated in Section 4.2, the concentrated phases for the boehmite dispersions to which the 186K PDMS is added are birefringent, whereas the boehmite dispersions to which 65K or 92K PDMS is added only give birefringent concentrated phases at the highest boehmite concentration. Given the fact that rodlike colloidal particles have a strong tendency to cluster under the influence of attractive forces, a possible explanation for the experimental observation might be that in the case of 65K and 92K PDMS the attractive depletion potential gives rise to clusters that do not have the capability to rearrange to a nematic ordering. Apparently, in the case of 186K PDMS, the attractive well is sufficiently broad to allow for nematic ordering. However, this is pure speculation and the elucidation of this problem awaits further experimental evidence.

6. CONCLUSION

We have performed phase separation experiments on a new composite liquid, containing rodlike colloidal particles and flexible polymer molecules, for two different length-to-diameter ratios of the rods in combination with different polymer sizes. For the short rods, two isotropic phases (dilute and concentrated) and a nematic phase could be identified in the phase diagram. These phases are observed to be in coexistence for a certain range of colloid and polymer concentrations. For the longer rods, a single isotropic phase

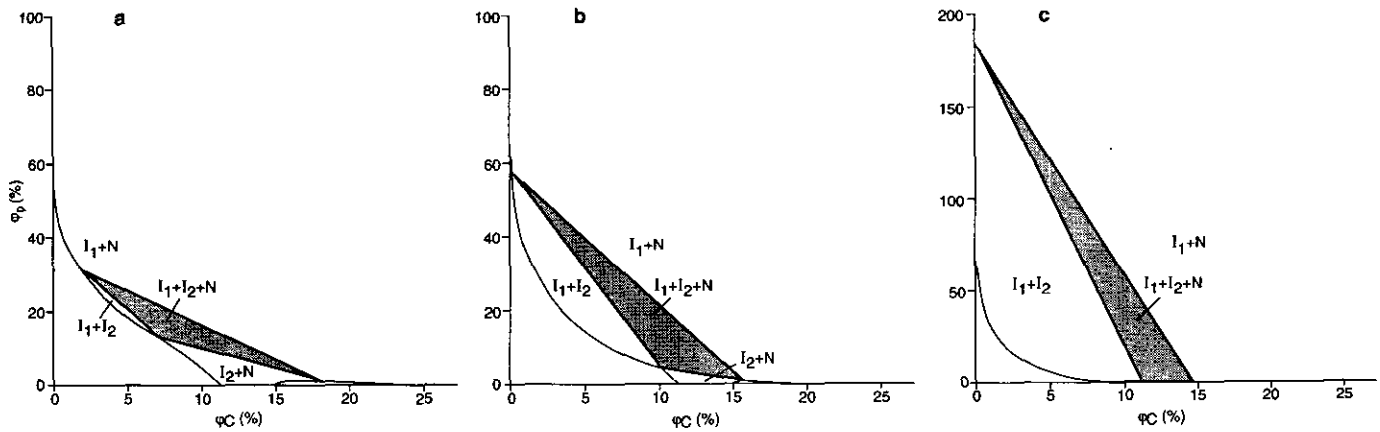

FIG. 11. Theoretical phase diagrams for a system of rodlike colloidal particles and flexible polymers (a) $\gamma = 27$ and $q = 2.5$ (b) $\gamma = 27$ and $q = 3.1$, (c) $\gamma = 27$ and $q = 4.8$.

and a nematic phase were observed. This qualitative difference in phase behavior as a function of the length-to-diameter ratio of the colloidal rods is in agreement with theoretical predictions recently obtained by two of us (37). In addition to the phases mentioned above, we also observed gel and/or glass states. The states that already occur at rather low colloid and polymer concentrations appear to be here even more prevalent than in the case of suspensions of spherical colloids with added flexible polymer.

Clearly more experiments on well-defined systems are required to elucidate the rich phase behavior of mixed suspensions consisting of rod-like colloidal particles and flexible polymer molecules. In particular, to reach an understanding of the gel and glass states reported here, further experimental and theoretical investigations are required.

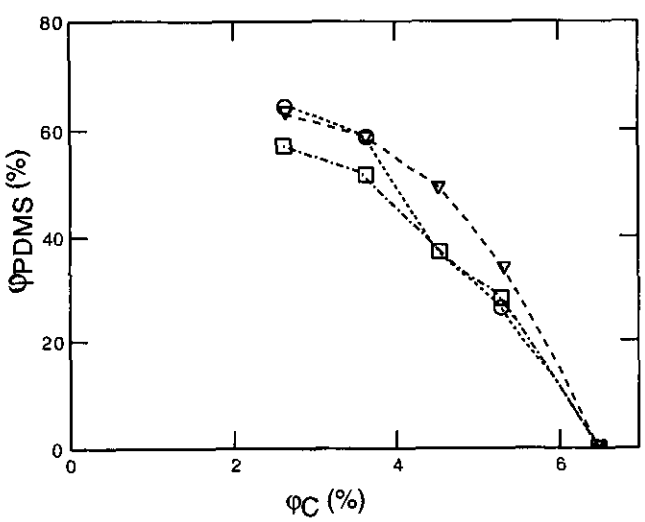

FIG. 12. Experimental phase diagrams from Fig. 9 replotted as a function of the effective polymer volume fraction ϕ_{PDMS}.

ACKNOWLEDGMENTS

We thank an anonymous referee for several worthwhile suggestions to improve the presentation of our work. We thank Marina Uit de Bulten and Hanneke de Vries for preparing the typescript and Jan den Boesterd for preparing the figures and photographs. This work was supported by the Netherlands Foundation for Chemical Research (SON) with financial aid from the Netherlands Organization for Scientific Research (NWO).

REFERENCES

1. Traube, J., *Gummi-Ztg.* **39,** 434 (1925).
2. Vester, C. F., *Kolloid Z.* **84,** 63 (1938).
3. Bondy, C., *Trans. Faraday Soc.* **35,** 1093 (1939).
4. Asakura, S., and Oosawa, F., *J. Chem. Phys.* **22,** 1255 (1954).
5. Asakura, S., and Oosawa, F., *J. Polym. Sci.* **33,** 183 (1958).
6. Sieglaff, C. L., *J. Polym. Sci.* **41,** 319 (1959).
7. Vrij, A., *Pure Appl. Chem.* **48,** 471 (1976).
8. de Hek, H., and Vrij, A., *J. Colloid Interface Sci.* **70,** 592 (1979).
9. Cowell, C., Li-In-On, R., and Vincent, B., *J. Chem. Soc., Faraday Trans. I* **74,** 337 (1978).
10. Vincent, B., Luckham, P. F., and Waite, F. A., *J. Colloid Interface Sci.* **73,** 508 (1980).
11. Feigin, R. I., and Napper, D. H., *J. Colloid Interface Sci.* **75,** 525 (1980).
12. Sperry, P. R., Hopfenberg, H. B. V., and Thomas, N. L., *J. Colloid Interface Sci.* **82,** 62 (1981).
13. de Hek, H., and Vrij, A., *J. Colloid Interface Sci.* **84,** 409 (1981).
14. Gast, A. P., Hall, C. K., and Russel, W. B., *J. Colloid Interface Sci.* **96,** 251 (1983).
15. Sperry, P. R., *J. Colloid Interface Sci.* **99,** 97 (1984).
16. Vincent, B., Edwards, J., Emmett, S., and Croot, R., *Colloids Surf.* **31,** 267 (1988).
17. Smits, C., van der Most, B., Dhont, J. K. G., and Lekkerkerker, H. N. W., *Adv. Colloid Interface Sci.* **42,** 33 (1992).
18. Liang, W., Tadros, Th.F., and Luckham, P. F., *J. Colloid Interface Sci.* **158,** 152 (1993).
19. Patel, P. D., and Russel, W. B., *J. Colloid Interface Sci.* **131,** 192 (1988).
20. Lekkerkerker, H. N. W., Poon, W. C. K., Pusey, P. N., Stroobants, A., and Warren, P. B., *Europhys. Lett.* **20,** 559 (1992).

21. Pusey, P. N., Poon, W. C. K., Ilett, S. M., and Bartlett, P., *J. Phys. Condens. Matter* **6,** A29 (1994).
22. Leal Calderon, F., Bibette, J., and Biais, J., *Europhys. Lett.* **23,** 653 (1993).
23. Cohen, S. S., *J. Biol. Chem.* **144,** 353 (1942).
24. Venekamp, J. H., and Mosch, W. H. M., *Virology* **22,** 503 (1964).
25. Leberman, R., *Virology* **30,** 341 (1966).
26. Yamamoto, K. R., Alberts, B. M., BVenzinger, R., Lawhorne, L., and Treibner, G., *Virology* **40,** 734 (1970).
27. Juckes, I. R. M., *Biochim. Biophys. Acta* **229,** 535 (1971).
28. Hwang, W.-F., Wiff, D. R., and Verschoore, C., *Polym. Eng. Sci.* **23,** 789 (1983).
29. Bianchi, E., Ciferri, A., Conio, G., Marsano, E., and Tealdi, A., *Macromolecules* **17,** 1526 (1984).
30. Marsano, E., Bianchi, E., Ciferri, A., Ramis, G., and Tealdi, A., *Macromolecules* **19,** 626 (1986).
31. Russo, P. S., and Cao, T., *Mol. Cryst. Liq. Cryst.* **157,** 501 (1988).
32. Huh, W., Lee, C. Y.-C., and Bai, S. J., *Polymer* **33,** 789 (1992).
33. Flory, P. J., *Macromolecules* **11,** 1138 (1978).
34. Pathmamanoharan, C., *Colloids Surf.* **34,** 81 (1988).
35. Buining, P. A., Pathmamanoharan, C., Jansen, J. B. H., and Lekkerkerker, H. N. W., *J. Am. Ceram. Soc.* **74,** 1303 (1991).
36. Buining, P. A., Veldhuizen, Y. S. J., Pathmamanoharan, C., and Lekkerkerker, H. N. W., *Colloids Surf.* **64,** 47 (1992).
37. Lekkerkerker, H. N. W., and Stroobants, A., *Il Nuovo Cimento,* in press.
38. Lekkerkerker, H. N. W., and Stroobants, A., "Complex Fluids" (L. Garrido, Ed.), Lecture Notes in Physics, Vol. 415, p. 1. Springer-Verlag, Berlin, 1993.
39. Reiss, H., Frisch, H. L., and Lebowitz, J. L., *J. Chem. Phys.* **31,** 369 (1959).
40. Cotter, M. A., *J. Chem. Phys.* **66,** 1098 (1977).
41. Brandrup, J., and Immergut, E. H., "Polymer Handbook," 3rd ed. Wiley, New York, 1989.
42. Berry, G. C., *J. Chem. Phys.* **44,** 4550 (1966).
43. Krigbaum, W. R., Carpenter, D. K., and Newman, S., *J. Phys. Chem.* **62,** 1586 (1958).
44. Buitenhuis, J., Dhont, J. K. G., and Lekkerkerker, H. N. W., *Macromolecules* **27,** 7267 (1994).
45. Buitenhuis, J., Thesis, Utrecht Univ., 1994.
46. Buining, P. A., and Lekkerkerker, H. N. W., *J. Phys. Chem.* **97,** 11510 (1993).
47. Pusey, P. N., Pirie, A. D., and Poon, W. C. K., *Physica A* **201,** 322 (1993).